International Journal of Engineering and Geosciences

https://dergipark.org.tr/en/pub/ijeg

e-ISSN 2548-0960

GIS-Based Geostatistical Techniques for Sedimentation Assessment Using USV Data: Case study Tuplang Reservoir, Uzbekistan

Khojiakbar Khasanov *, Masharif Bakiev

"Tashkent Institute of Irrigation and Agricultural Mechanization Engineers" National Research University, Tashkent, Uzbekistan, admin@tiiame.uz

Cite this study: Khasanov, Kh. & Bakiev, M., (2025). GIS-Based Geostatistical Techniques for Sedimentation Assessment Using USV Data: Case study Tuplang Reservoir, Uzbekistan. International Journal of Engineering and Geosciences, 10 (2), 231-243.

https://doi.org/10.26833/ijeg.1567019

Keywords
Tupolang reservoir
Bathymetric survey
USV Apache3
Geostatistical analysis
3D model
Sedimentation capacity volume reduction

Research/Review Article

Received:14.10.2024
Revised: 09.01.2025
Accepted:17.01.2025
Published:01.07.2025

Abstract

This study investigates the impact of sedimentation on the storage capacity of the Tupalang Reservoir, located in Surkhandarya, Uzbekistan, over a period of more than 30 years. Sedimentation poses a significant challenge by gradually reducing reservoir capacity, affecting water availability for irrigation, hydropower, and drinking supply. In the study, sedimentation was evaluated using GIS-based geostatistical methods using USV data in the reservoir. For the bathymetric data processing that was collected in 2023, four interpolation techniques—IDW, RBF, OK, and EBK —were applied, with RBF demonstrating the highest predictive accuracy. Results indicate a capacity loss of 28.05 million cubic meters (Mm^3), or 5.65% of the total volume, primarily in the dead storage zone between 830 m and 890 m above sea level. Using bathymetric surveys conducted in 2003, 2007, 2010, and 2023, this research assesses changes in reservoir volume and identifies sedimentation patterns. The findings highlight a decline in sedimentation rates from 1.51 Mm^3 per year in the early years to 0.3 Mm^3 per year after 2010, attributed to effective management practices such as hydraulic washing. The study underscores the importance of proactive sediment management strategies, including dredging and sediment traps, to sustain reservoir functionality and recommends ongoing monitoring using advanced geospatial techniques.

1. Introduction

The unique geographical features of Central Asia (CA), such as its moderate climate and diverse landscapes, have historically shaped economic activities like irrigated agriculture and livestock breeding [1]. The economy of CA heavily relies on irrigated agriculture, particularly the Amu Darya and Syr Darya rivers. In the CA, Soviet-era infrastructure still affects water distribution and management [2-3]. Reservoirs are pivotal in managing water resources, facilitating irrigation, and supporting hydropower generation in the region [4].
Climate change impacts, coupled with population growth, are anticipated to affect water reservoir performance, emphasizing the need for reliable and resilient water management strategies [5]. One of the prerequisites for formulating a management strategy for water reservoirs is the accessibility of data regarding their capacity volume. Precise reservoir capacity volume information is attainable through design specifications or the most recent bathymetric survey findings [6,7]. However, the capacity volume changes due to sedimentation over several years of operation. Sedimentation poses a significant challenge to reservoir functionality and capacity volume of reservoir [8,9].

Sediment accumulation, practiced by factors like changing hydrological conditions and land use practices, leads to a gradual decrease in capacity volume, impacting water management, flood control, and energy production [10]. Sedimentation in reservoirs primarily stems from several factors such as land use changes, climate change impacts, and anthropogenic activities like overgrazing and deforestation [11,12]. These activities lead to increased sediment loads in rivers, gradually accumulating behind dams [13]. Reservoir sedimentation poses challenges for water management, flood control, and energy production [14]. The sedimentation process is complex, influenced by factors like reservoir bottom shapes, sediment textures, and river discharges [15]. Sediment in reservoirs commonly exists in both dissolved and solid forms, exhibiting properties of non-cohesive and cohesive materials. Sedimentation rates vary significantly by region. Some regions, particularly those with high erosion rates, experience more rapid sedimentation in reservoirs [16].

The rate at which capacity volume diminishes is contingent upon several factors, including the sediment yield of the river upon which the reservoir is constructed, the morphological characteristics of the reservoir, and the operational framework of the project [17,18]. The determination of reservoir capacity volume loss and periodic sedimentation rates relies on historical and new bathymetric survey data or assessments of sedimentation status [19,20]. Determining the size of water reservoirs is especially important for Uzbekistan, especially during the drought of recent years. It is considered one of the main factors in the proper distribution of available water, estimation of electricity production and most importantly in developing dam safety criteria. Sediment accumulation in reservoirs poses significant challenges for water management, flood control, and energy production. This means that such reservoirs will lose half of their capacity in 25-50 years, and in 50-100 years they will completely silt up and fail. Figure 1 below shows capacity volume loss due to sedimentation in some reservoirs in the Republic. Bathymetric surveys were conducted by the Bathymetric Center under the Ministry of Water Resources of Uzbekistan during 2000–2006. The surveys used a moving boat equipped with GPS, an electronic depth sounder, and an automatic data recorder (CEEDUCER®). Depths were calculated by subtracting the depth device constant from the water surface elevation, synchronized with positional data to map the reservoir basin. The basin profile was generated in a specialized program, and reservoir volumes were calculated from these profiles. However, this process was time-consuming and yielded moderate accuracy.

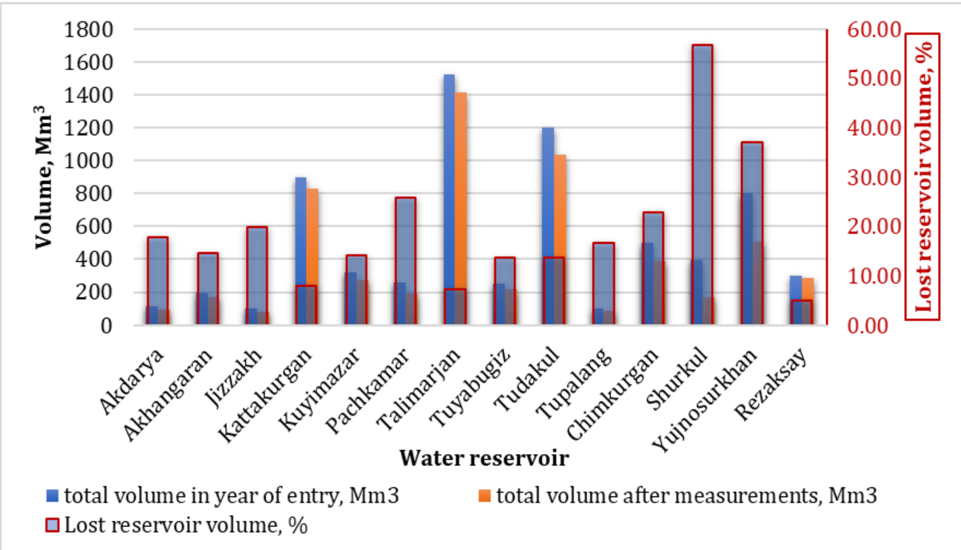

Figure 1. Decrease in total and dead volume capacities due to sedimentation in some reservoirs in Republic of Uzbekistan.

Bathymetric surveying of reservoirs involves measuring water depth and sedimentation to assess storage capacities and water quality [21,22]. Various methods like satellite bathymetry, sonars, and echo sounders are utilized for this purpose [23].

In recent years, the application of Geographic Information Systems (GIS) and Remote Sensing (RS) has significantly enhanced the management of reservoirs, providing valuable tools for monitoring, planning, and optimizing their use. These technologies play a crucial role in various aspects of reservoir management, from sedimentation control and flood risk assessment [24] to water quality monitoring, operational optimization, site selection for new reservoirs [25,26], coastal erosion and sediment accumulation [27], watershed management and environmental impact evaluation [28,29]. Including, modern techniques, such as using hydrographic survey boats equipped with SONAR devices and GIS software, provide accurate and cost-effective ways to quantify reservoir storage capacities [30].

The research's primary objective is to investigate how the Tupalang reservoir's dead volume and total capacity volume have changed during its years of operation. In the implementation of the research, the data of the bathymetric research conducted in the water reservoir was used. Bathymetric data were processed by geostatistical analysis.

2. Study Area

The toppling Reservoir, situated on the Tupalang Darya River within the Sariasi district of the Surkhandarya region, is characterized by its geographical boundaries. To the west, it is delimited by the Surkhantau ridge, while to the east, it is bordered by the Machetli southern spurs, located in the western region of the Gissar ridge. The catchment area of the Tupalang reservoir is 3080 km^2, and the weighted average height of the catchment is 2270m (Figure 2). The construction of the Topalang Reservoir started in 1980 and was completed in 1994, with the gradual commissioning of the Topalang Hydroelectric Power Plant. The first power unit, with a 30 MW capacity, was commissioned in 2006, followed by a second phase in 2023 that added a 145 MW capacity, making each unit capable of generating 72.5 MW of electricity.

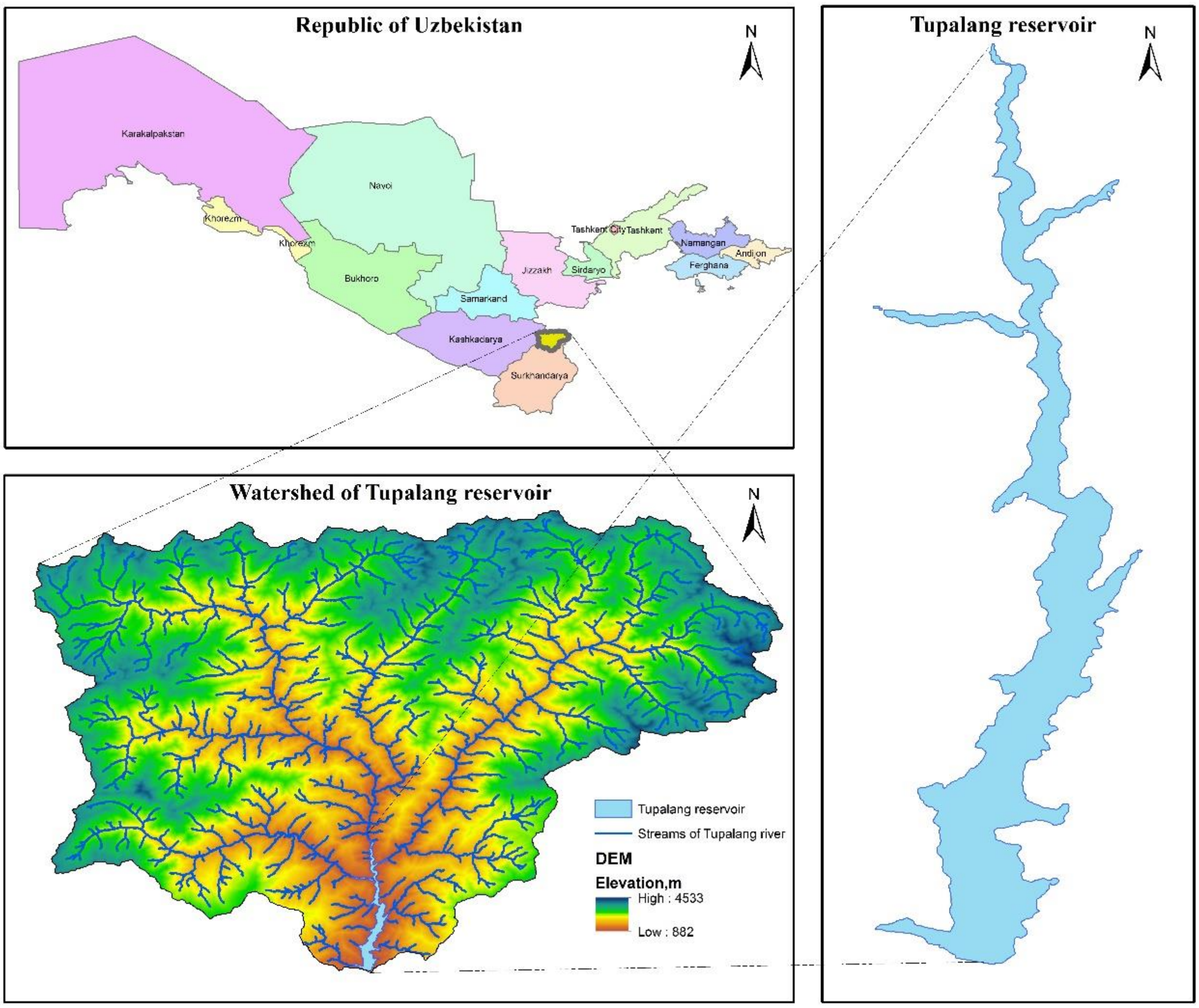

Figure 2. Location of Topalang Reservoir.

As a Class I structure, the Tupalang Reservoir is a critical element of the region's infrastructure, significantly contributing to addressing water shortages and energy demands. Furthermore, the construction of a 361-kilometer main water pipeline from the reservoir began in September 2021, aimed at supplying drinking water to 1.7 million people across Sariosia, Denov, Shorchi, Kumkurgan, Zharkurgan, Bandikhon, Kyzyriq, Sherabad, Angor, Muzrobod, and Termiz districts, including Termiz, the regional center. The Tupalang Reservoir has thus emerged as a key factor in the socio-economic development of the Surkhandarya region, serving as a vital resource for energy production, water supply, and regional growth.

2.1. Climate

The climate in the plain areas of Surkhandarya region is arid, with significant annual and daily temperature fluctuations. In winter and transitional periods, weather conditions are heavily influenced by cyclones from the southern Caspian Sea and the upper reaches of the Tejen and Murgab rivers. The powerful mountain ranges in the eastern part of the region create diverse climate patterns, causing variations in temperature and precipitation. These ranges, which intercept moist air masses, intensify weather fronts and lead to significant localized moisture. The average annual temperature is 15.7°C, with extremes reaching as high as +47°C and as low as -25°C. Temperature distribution across the region varies due to rugged terrain and considerable elevation differences. Relative humidity ranges from 47-58%, lowest in summer and highest in January, with high temperatures combined with low humidity causing air dryness. The annual precipitation is 360 mm, peaking in March-April while the summer months are dry. Mountain systems significantly influence wind patterns, creating local circulations and seasonal wind variations; in the cold season, northeasterly winds predominate at speeds of 2-4 m/s. The annual evaporation rate is 1374 mm.

3. Materials and methods

3.1. Bathymetric surveying of Tupalang reservoir

The bathymetric survey of the Tupalang Reservoir utilized single-beam and broadband echo sounders with acoustic pulse systems, alongside geodesic shoreline surveys, conducted in multiple stages for comprehensive data collection and analysis.

In 2023, LLC "Center for Safety Assessment and Monitoring of Hydrotechnical Facilities" ("HYDROTECHMANITORING") carried out a bathymetric survey of the Tupalang Reservoir using the USV Apache3, Chcnav i90 GNSS, Leica TS 09 electronic tachymeter, and Trimble Dini 0.3. Prior to the survey, the APACHE 3 USV underwent a thorough evaluation, confirming its precision within a range of ±1, ensuring the reliability and accuracy of the bathymetric data collected.

USV Apache3: A versatile unmanned surface vehicle (USV) designed for conducting hydrographic surveys and water-based data collection. It is equipped with sensors and GPS for precise positioning and data acquisition.

Chcnav i90 GNSS: A high-precision GNSS (Global Navigation Satellite System) receiver used for accurate positioning and surveying. It provides real-time corrections for geospatial data collection, ensuring reliable coordinates in challenging environments.

Leica TS 09 Electronic Tachymeter: A high-precision total station used for measuring angles and distances in surveying. It is commonly used in land and water surveying for topographic mapping and geospatial data collection.

Trimble Dini 0.3: A high-performance depth sensor or echo sounder, often used in bathymetric surveys. It measures the depth of water bodies with high accuracy, helping to map the underwater topography.The reservoir under study spans an area of 8.85 km^2, with a width varying from 200 to 1200 m, and a length exceeding 14 km. The boundaries of the reservoir and the flight path of the UAV, consisting of 106 cross-sections, were established using the Autoplaner application and an online map. In addition, the topographic survey of the banks was conducted to enhance the accuracy of the bathymetric model of the reservoir (Figure 3).

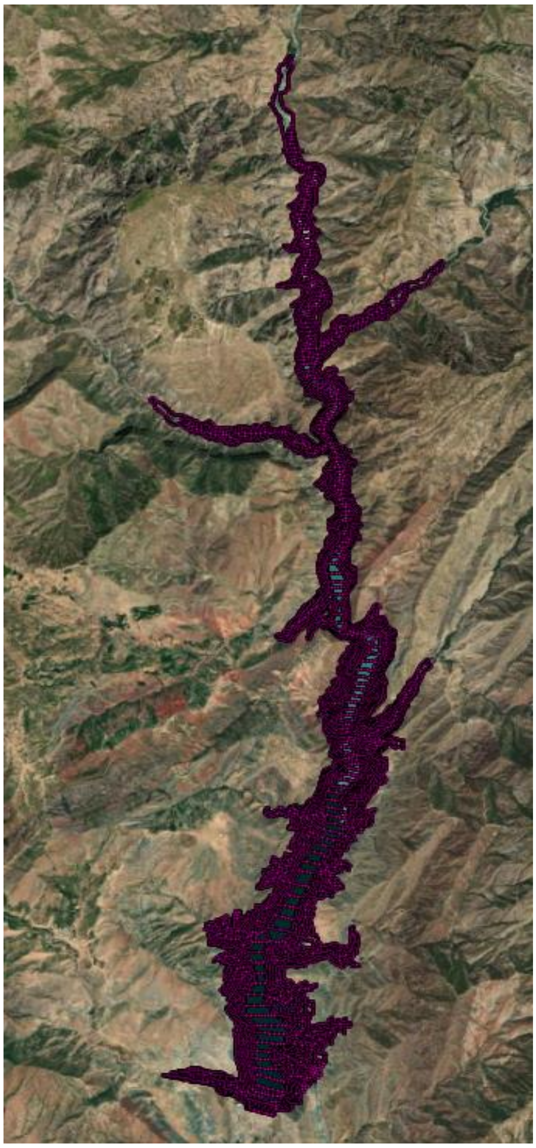

Figure 3. Collected measured topo-bathymetric data during Tuplang reservoir survey.

3.2. Bathymetric data processing

Bathymetric data processing involves various methods to analyze and interpret underwater depth information. Different studies highlight the significance of data reduction techniques for efficient analysis and visualization of bottom surfaces [31]. In their research, Claudio Parente and Andrea Vallario used interpolation methods such as Radial Basis Function and Kriging to process single beam echo sounder data to create accurate 3D bathymetric models [32]. To estimate reservoir shape and compute water volume, a few researchers processed bathymetry data using wavelet decomposition, interpolation techniques, and 3D modeling [33,34].

In processing UAV and USV data and evaluating the accuracy of topographic or bathymetric maps created on the basis of this data, research results are positively affected [35].

Therefore, in this study, two deterministic methods (inverse distance weighting and radial basis function) and two geostatistical techniques (Ordinary Kriging and Empirical Bayesian Kriging) were tested and evaluated in the processing of USV data collected in Tupalang Reservoir, because the field measurement work consisted of both underwater and dry parts, as the sample density was different.

3.2.1. Inverse Distance Weighting (IDW)

IDW interpolation is a deterministic technique used to estimate values at locations where data is not observed. It calculates the value of an unknown location by comparing it to the values of nearby locations [36]. IDW assigns weights to the nearby locations based on their distance from the interpolated point, with closer locations having higher weights. The weighted values are then used to estimate the value at the unknown location. The values of the variable of interest to be interpolated are denoted by $\hat{Z}$ and are evaluated by the following Equation 1 [37]:

$$\hat{Z}(x,y) = \sum_{i=1}^{N} W_i(x,y) Z_i \quad (1)$$

Where: Wi - the weight for each observation and is expressed as Equation 2:

$$W_i(x,y) = \frac{d_i(x,y)^{-p}}{\sum_i^N d_i(x,y)^{-p}} \quad (2)$$

p is the positive power parameter (The higher the value of p, the more the weights are influenced by the inverse of the distances raised to the power p)

d_i - is the distance between the prediction location and the sampled point and is defined as follows Equation 3:

$$d_i(x,y) = \sqrt{(x-x_i)^2 + (y-y_i)^2} \quad (3)$$

3.2.2. Radial Basis Function (RBF)

RBF interpolation is a powerful deterministic method in geostatistics and GIS, commonly applied to smooth scattered data and estimate values at unsampled locations by using observed data points, with additional applications in interpolating implied volatility surfaces in financial modeling [38]. There are several basic functions used in interpolation, including the thin-plate spline, spline with tension, completely regularized spline, multiquadric function, and inverse multiquadric spline [39]. Bishop's book [40] is recommended one common form of the RBF interpolation Equation 4 is:

$$K(x,y) = e^{(-\sigma\|x-y\|^2)} \quad (4)$$

Where: σ - is a parameter that controls the width of the Kernel, $\|x-y\|$ - the Euclidean distance between the prediction location and the sampled point

3.2.3. Ordinary kriging interpolation (OK)

OK - is a geostatistical interpolation method used for estimating values at un-sampled locations based on the observed values at sampled locations. It incorporates spatial autocorrelation, considering not only the distances between sample points but also the spatial structure or variability in the dataset. The Ordinary Kriging interpolation Equation 5 is as follows [41]:

$$\hat{Z}(S_0) = \sum_{i=1}^{N} \lambda_i Z(S_i) \quad (5)$$

Where: $Z(s_i)$ = the measured value at the i^{th} location, λ_i = an unknown weight for the measured value at the i^{th} location, s_0 = the prediction location, N = the number of measured values

The empirical variogram is calculated from the data to explore the spatial dependence and serves as a basis for fitting theoretical models such as spherical, exponential, and Gaussian variograms [42].

3.2.4. Empirical Bayesian Kriging (EBK)

EBK is a geostatistical interpolation method that combines the principles of kriging with a Bayesian approach to estimate variogram parameters [43]. Unlike traditional kriging, which requires prior knowledge or assumptions about the variogram, EBK uses observed data to infer the variogram characteristics [44]. Variograms are calculated based on the Equation 6 [45]

$$\gamma(\mathrm{h}) = \frac{1}{2n} \sum_{i=1}^{n} \{Z(xi) - Z(xi+h)\}^2 \quad (6)$$

Where: h – distance, Z - different values, n - number of data samples

3.2.5. Cross-validation statistics criteria

The evaluation of interpolation techniques is typically conducted using cross-validation statistical criteria, including root mean square error (RMSE), mean absolute error (MAE), coefficient of determination (R^2), and standard error of prediction (SEpred), to assess and compare the performance, accuracy, and reliability of different methods for robust predictive analysis [46,47]. Cross-validation is a widely adopted and effective statistical practice for this purpose [48]. It allows for the estimation of model performance by assessing how well the model generalizes to new data that was not used in training [49]. By using cross-validation, the models' ability to capture both variance and bias can be evaluated, as no single metric can adequately capture both [50]. By comparing interpolation techniques through cross-validation, an effective and widely adopted statistical practice, a comprehensive assessment of the models' predictive capabilities is achieved. Table 1 below presents the main objectives of using RMSE, MAE, R^2, and SEpred, along with their corresponding equations and value ranges.

Table 1. Tabular comparison of RMSE, MAE, R2, and SDpred.

Metric	Formula	Reason for use	Range of Values
RMSE	$\mathrm{RMSE} = \sqrt{\frac{\sum_{i=1}^{n}(P_i - M_i)^2}{n}}$	Provides a measure of how well the model captures the spatial distribution of the bathymetric data. It is sensitive to the magnitude of errors, making it useful for understanding the overall fit.	from 0 to ∞ *As low as possible. Lower values indicate better model performance.*
MAE	$\mathrm{MAE} = \frac{\sum_{i=1}^{n}\lvert P_i - M_i\rvert}{n}$	Useful for understanding the average magnitude of errors in the 3D model. Particularly relevant to minimize the impact of extreme values in assessment.	from 0 to ∞ *As low as possible. Lower values indicate better model performance.*
R²	$R^2 = \left(\frac{\frac{1}{n}\sum_i^n (M_i - M_m)(P_i - P_m)}{\sqrt{\frac{1}{n}\sum_i^n (M_i - M_m)^2}\sqrt{\frac{1}{n}\sum_i^n (P_i - P_m)^2}}\right)^2$	A higher R² suggests a better fit, indicating how much of the variance in the data is accounted for by the 3D model	0 to 1 *Close to 1. A higher R² indicates a better fit.*
SE$_{pred}$	$SE_{pred} = SD\sqrt{(1 - R^2)}$	SEpred provides a measure of the uncertainty associated with the interpolated or predicted bathymetric values.	from 0 to ∞ *SEpred value of zero would imply perfect precision, meaning that the predictions match the observed values exactly.*

In the above equations: M_i and P_i represent, respectively, the ith measured and predicted values for n observations. M_m and P_m are, respectively, the mean values of Mi and Pi.

4. Results

4.1. Results of the chosen interpolation methods

Field surveys within the Gissarak reservoir encompassed both underwater and dry sections, leading to variations in sampling densities. To effectively interpolate data and generate comprehensive representations, four distinct techniques were employed: RBF, IDW, OK and EBK. The performance of these interpolation methods was rigorously evaluated based on statistical criteria of verification, including RMSE, MAE, R^2 and SEpred.

For the RBF interpolation, ArcGIS 10.8.2 software was employed to optimize kernel parameters, selecting "Multiquadric" as the kernel function, with s=0.31 determined via cross-validation, a neighbor range of 8 to 64, and both the major and minor semiaxes set equally under a one-sector configuration.

The IDW interpolation method was implemented using the same software, focusing on tuning the optimal search radius and power values (p) as specified by Eq. (3), with optimal results achieved by adjusting the power parameter between 1 and 3, ultimately increasing it to 8 for fine-tuning; the number of neighboring points in the search radius was set to a maximum of 50 and a minimum of 5, with the sector type configured to 1 sector.

OK employed three variogram models—spherical, exponential, and Gaussian—to fit the spatial variations from the topo-bathymetric surveys, selecting the most suitable variograms through the optimization of variogram parameters and performance criteria via cross-validation. Table 5 presents the ranges of increments that define the appropriate variograms for the reservoir, with a steering angle of 45°, while the number of neighboring points in the search radius was set to a maximum of 50 and a minimum of 5, utilizing the standard neighborhood type and an 8-sector configuration.

(EBK) method was applied to optimize the kernel parameters as defined by Eq. (6), with the number of neighboring points in the search radius set to 64, while the search radius itself allowed for a maximum of 50 and a minimum of 5 neighboring points, utilizing the standard neighborhood type and an 8-sector configuration, with a total of 100 simulations conducted. The optimal reservoir results are recorded in Table 2.

Table 2. Results of the chosen interpolation methods

Metric	RMSE	MAE	R^2	SDpred
IDW	2.45	0.019	*0.976*	*2.32*
RBF	1.61	0.008	*0.997*	*1.57*
OK	1.51	0.009	*0.994*	*1.56*
EBF	1.54	0.009	*0.993*	*1.59*

The table compares the performance of four interpolation methods—IDW, RBF, OK, and EBF — based on key metrics: RMSE, MAE, R^2, and SDpred. Among the methods, RBF has the lowest RMSE (1.61) and MAE (0.008), along with the highest R^2 (0.997), indicating superior accuracy and predictive performance. OK follows closely, with slightly higher RMSE (1.51) and MAE (0.009) but also performs well in terms of R^2 (0.994). EBF and IDW show higher error values and lower R^2, with IDW performing the least accurately based on all metrics. Overall, RBF and OK demonstrate better precision in the interpolation process compared to IDW and EBF.

The best result was obtained using the RBFs method (Figure 4).

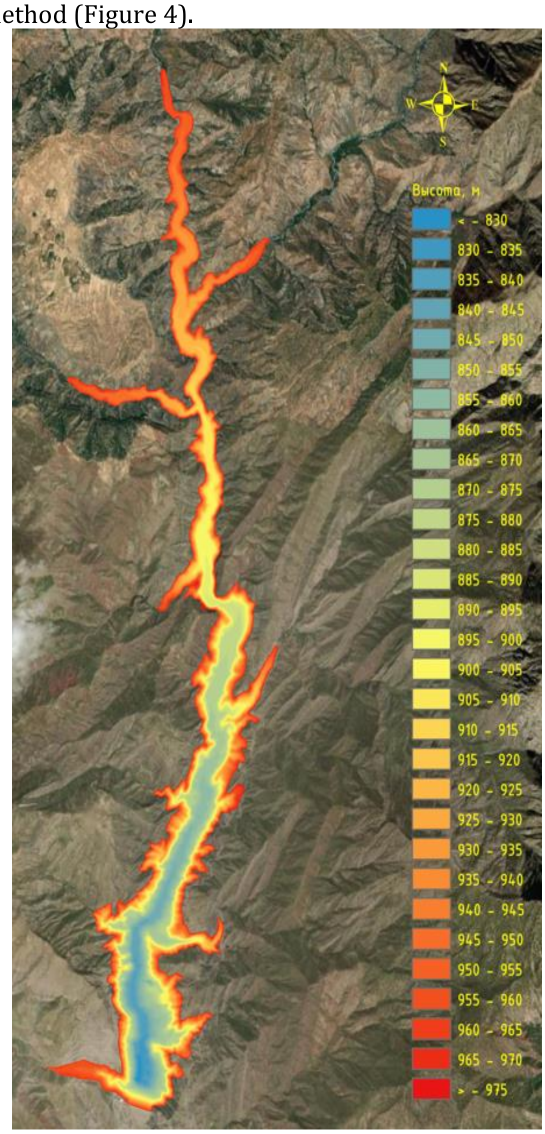

Figure 4. Bathymetric model of the reservoir bowl created using the RBF method (2023).

By modeling bathymetry, researchers have proposed that they can calculate reservoir capacity volumes and create 3D models that facilitate capacity volume estimation [51,52]. A 3D model of the Tupalang reservoir was developed based on the spatial model obtained based on the RBFs method (Figure 5).

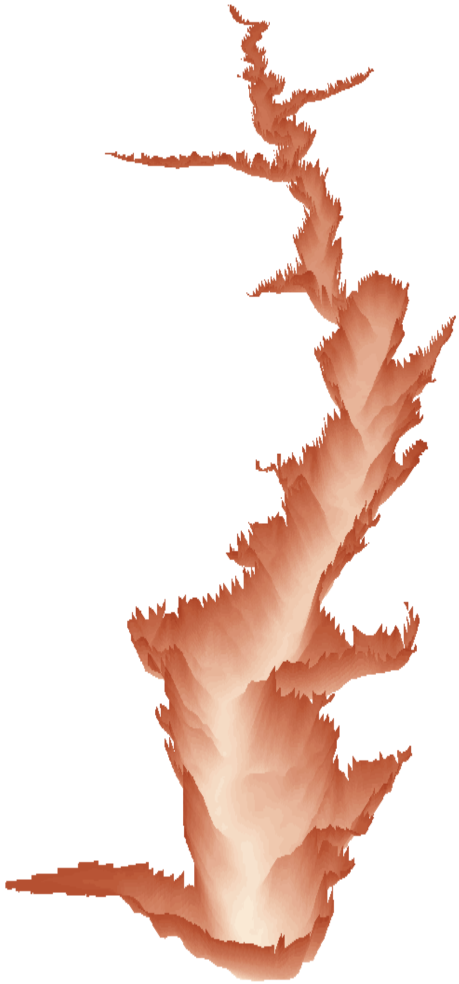

Figure 5. 3D model of the reservoir bowl (2023)

4.2. Tupalang reservoir water storage

The "Function Storage Capacity" tool of the ArcGIS program calculates storage area capacities and volumes based on input stage heights, with the option to use a mask for limiting locations. It presents a table of total storage area and capacities with step marks and generates a summary report including tool parameters, a map of the study area, and storage capacity tables and graphs. Users can select the desired stage height by adjusting parameters such as maximum (960), minimum (828), and incremental values (1m). The z-factor ensures accurate storage capacity calculation when surface z units differ from ground x and y units.

The total volume of Tupalang Reservoir was 468.27 Mm^3, and the reservoir surface area was 8.34 km^2 at FSL (960 m.a.s.l.). The Surface area - elevation and capacity volume - elevation relationships play a crucial role in reservoir analysis, sediment prediction, and understanding seasonal water storage variations [53,54]. The obtained results are presented in Figure 6 in the form of "Area elevation curve and capacity volume elevation curve".

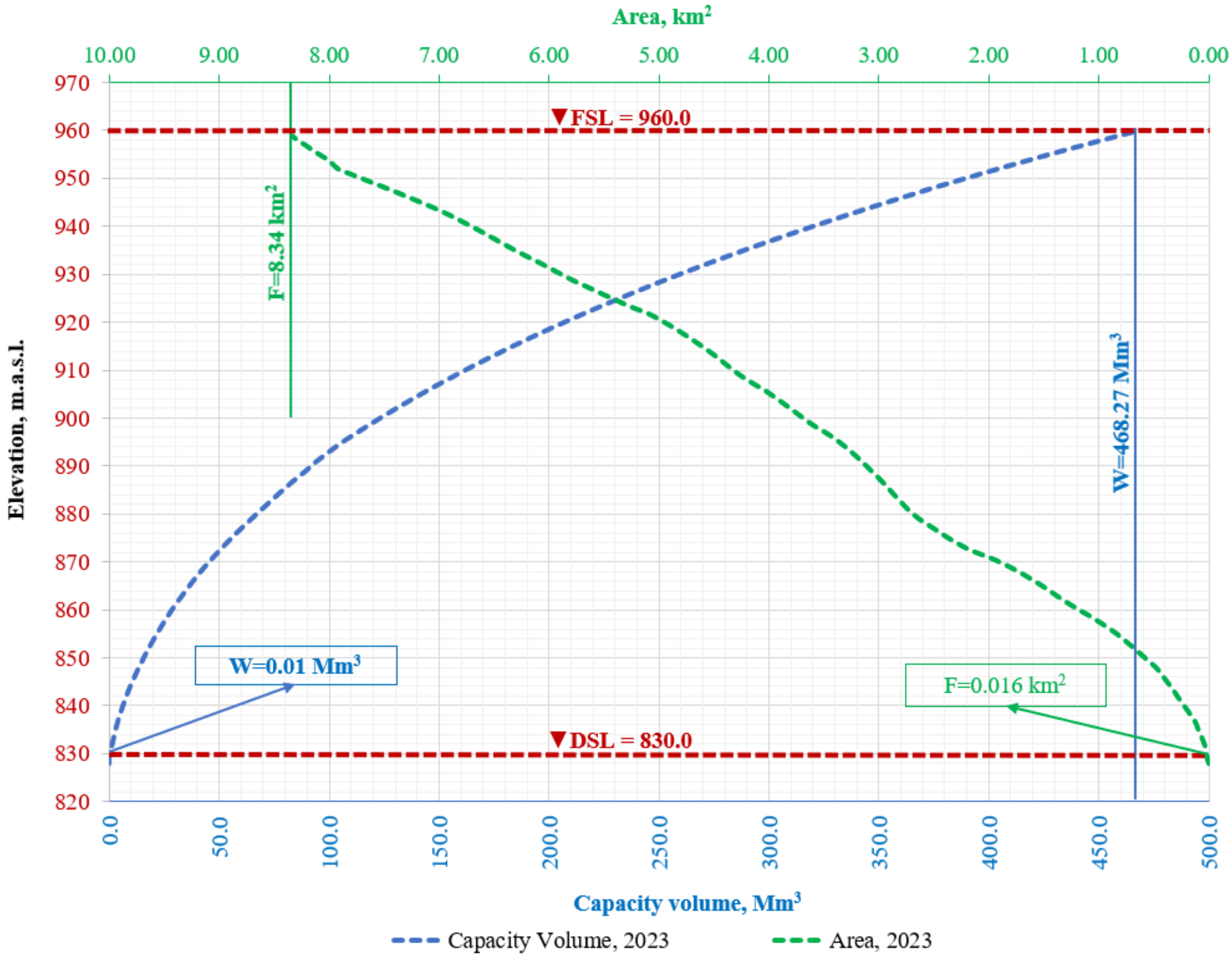

Figure 6. Surface area - elevation and capacity volume - elevation curve

4.3. Totaling reservoir sediment storage

The comparison of recent bathymetric survey results with the original design parameters of the water reservoir revealed significant sedimentation over a 30-year operational period. The analysis indicated that the volume of sedimentation amounted to 28.05 Mm^3, constituting approximately 5.65% of the reservoir's total capacity volume. Additionally, this sedimentation led to a reduction in the reservoir's surface area by 0.1 square kilometers.

The analysis of capacity volume changes in levels indicates that sedimentation has reached a critical point, with the sediment level reaching 830 meters above sea level (masl). This signifies that the dead volume of the reservoir is now filled with sedimentation. Sedimentation processes within the reservoir occurred between the levels of 830 masl and from 888 to 890 masl (Figure 7). This distribution is attributed to the dead level being situated at 830 masl, while the water inlet to the reservoir, particularly in the initial stage, is positioned at 890 masl. Operational experience underscores that the primary sedimentation processes typically occur at the reservoir inlet and more at the dead level.

The findings of the analysis underscore the critical state of sedimentation within the reservoir, with the dead volume now completely filled with sediment. Admittedly, Sediment accumulation, a natural process occurring over time, has reduced the reservoir's ability to store water effectively. However, this reduction in capacity volume can have implications for various water management activities, including water supply, irrigation, hydropower generation, and ecosystem services. This highlights the urgent need for intervention to mitigate further sedimentation and preserve the reservoir's functionality. To address this issue, it is essential to implement sediment management strategies, such as dredging or sediment traps, to prevent further accumulation and maintain water storage capacity.

In addition to the bathymetric survey conducted in 2023, several were conducted in the Tupalang Reservoir, including those in 2003, 2007, and 2010, to assess turbidity deposition and its impact on the reservoir's capacity volume (Figure 8).

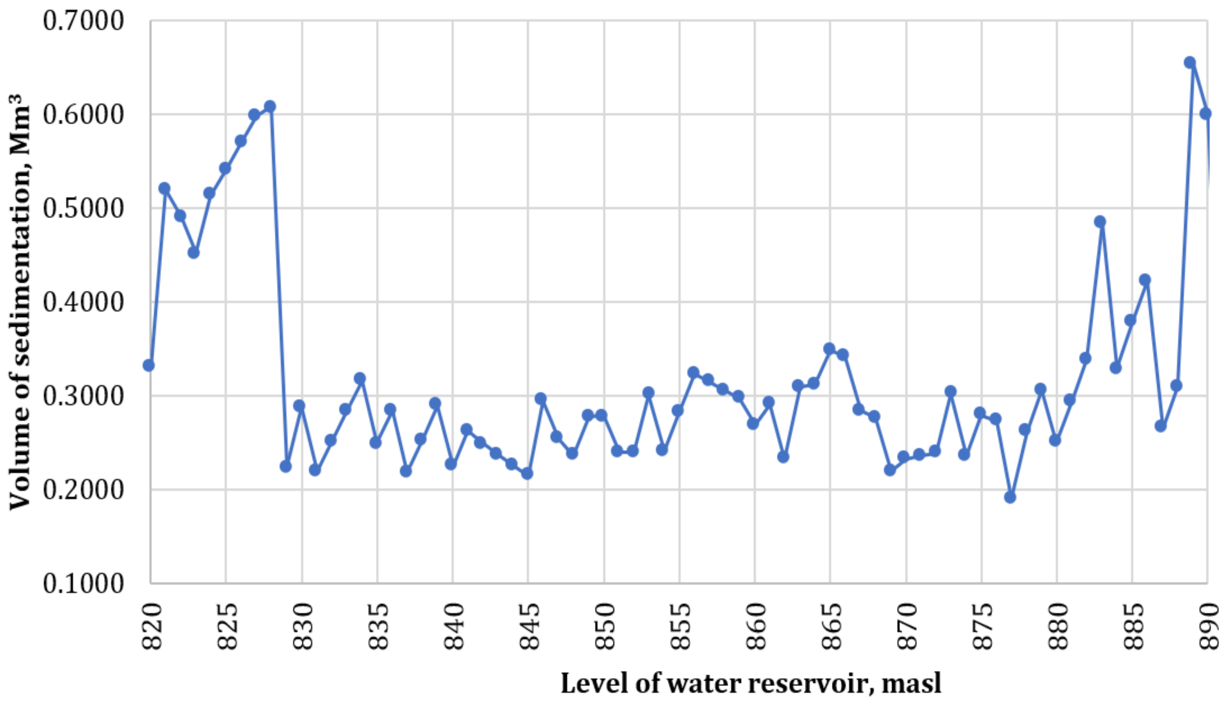

Figure 7. Curves of the dependence of reservoir capacity volume on water levels (1980 and 2023)

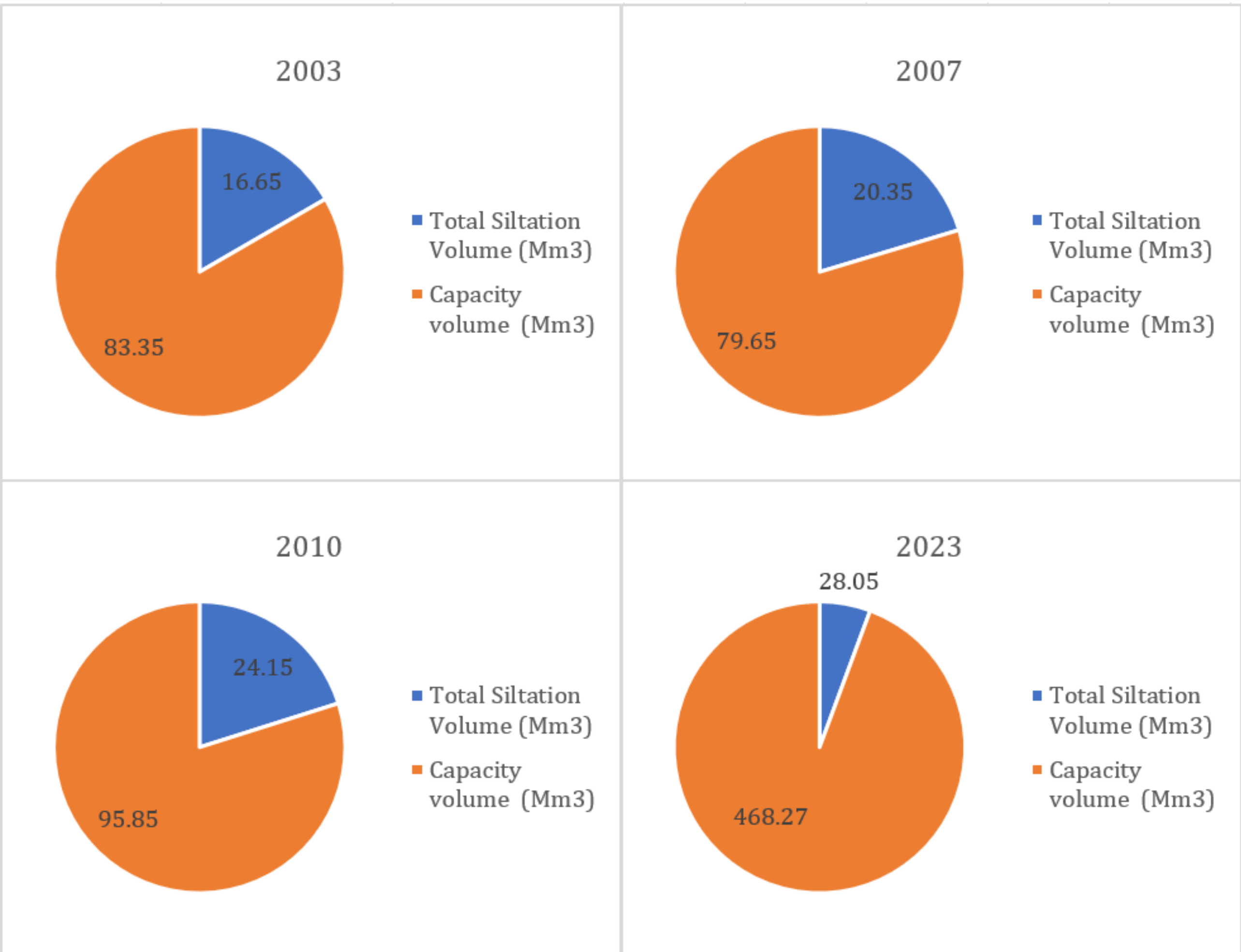

Figure 8. The results of bathymetric surveys conducted in different years determined the volume of sedimentation and the capacity volume of the reservoir.

As previously noted, the reservoir's capacity volume was 100 Mm³ until 2007, increased to 120 Mm³ by 2010, and expanded further to approximately 496.32 Mm³ by 2020. Table 3 presents a summary of the bathymetric analysis results.

Table 3. The analysis of results of bathymetric surveys conducted in different years.

Period	Years	Total capacity volume (Mm3)	Capacity volume loss (Mm^3)	Percentage of total capacity volume	Sediment volume in the period	Anual Sediment volume (Mm^3)
1st Period	1992–2003	100	16.65	16.65%	16.65	1.51
2nd Period	2003–2007	100	20.35	20.35%	3.7	1.05
3rd Period	2007–2010	120	24.15	20.13%	3.8	1.08
4th Period	2010–2023	496.23	28.05	5.65%	3.9	0.3

By analyzing the results of all bathymetric studies, an examination of the capacity volume loss of the reservoir during the exploitation period was conducted. The bathymetric survey was partitioned into distinct periods based on years.

First period (1992-2003). Findings from the 2003 bathymetric research revealed a capacity volume loss of 16.65 Mm³ due to sediment deposition, constituting 16.65% of the total capacity volume. This translates to an average annual loss of 1.51 Mm³.

Second period (2003-2007). The 2007 bathymetric survey identified 20.35 Mm³ (20.35% of the total capacity volume) of silt sediment in the reservoir, indicating a capacity volume loss of 3.7 Mm³ over 3.5 years, equivalent to an annual average of 1.05 Mm³.

In the third period (2007-2010), with the reservoir capacity volume at 120 Mm³ in 2010, the bathymetric survey revealed 24.15 Mm³ (20.13% of the total capacity volume) of turbid sediment. This denotes a capacity volume loss of 3.8 Mm³ over 3.5 years, averaging 1.08 Mm³ per year. Additionally, a sediment level was recorded at 830 masl, indicating the complete filling of the reservoir's dead volume with muddy sediments.

In the fourth period (2010-2023), with the reservoir capacity volume reaching 496.23 Mm³ by 2020, the 2023 bathymetric research determined 28.05 Mm³ of mud sediment, accounting for 5.65% of the total volume. The reservoir experienced a capacity volume loss of 3.9 Mm³ between 2010 and 2023, averaging 0.3 Mm³ per year. This notable decrease can be attributed to the removal of muddy sediments from the reservoir by hydraulic washing following the filling of the dead volume in 2010

The analysis indicates consistent average volume loss in the second and third periods, a comparatively higher loss in the first period, and a substantial reduction in the fourth period. The initial abundance of turbid sediments observed in the first period, evidenced by the displacement of grunts during reservoir filling, stabilized in subsequent periods. The significant decrease in volume loss in the fourth period can be attributed to the removal of muddy sediments through hydraulic washing following the complete filling of the reservoir's dead volume in 2010.

5. Conclusion

This research aimed to analyze changes in the dead and total capacity volumes of the Tupalang Reservoir over 30 years using bathymetric survey data. Four interpolation methods—IDW, RBF (deterministic), and OK, EBF (geostatistical)—were evaluated based on statistical criteria such as RMSE, MAE, R^2, and SEpred to assess their performance and accuracy in predictive analysis. .

The results showed that the RBF method outperformed the others, with the lowest RMSE (1.61), MAE (0.008), and the highest R^2 (0.997). Ordinary Kriging had slightly higher RMSE (1.51) and MAE (0.009) but still achieved a strong R^2 of 0.994. In comparison, the IDW method had higher error values and lower R^2, making it the least effective. These findings highlight the importance of choosing the right interpolation method for reliable and accurate spatial models in hydrological studies. A 3D model of the Tupalang Reservoir, created using the RBF method, was developed to visualize sedimentation patterns and capacity changes. .

The analysis reveals a notable decrease of 28.05 million cubic meters (Mm^3) in the Tupalang Reservoir's capacity, primarily due to natural processes and human activities influencing sediment accumulation. Sedimentation is occurring at an average rate of 0.3 Mm^3 per year, a small proportion of the reservoir's total capacity of about 500 Mm^3. This suggests that effective reservoir management and flow regulation have helped reduce sedimentation impacts. While sedimentation is a natural and inevitable process, strategies like dredging, sediment traps, and watershed management can significantly reduce sediment inputs and mitigate its effects, ensuring the reservoir's continued functionality for water storage and irrigation.

Acknowledment

LLC "Center for Safety Assessment and Monitoring of Hydrotechnical Facilities" generously contributed bathymetric data. The authors would like to express their gratitude to all members of the hydrographic survey crew who assisted them with this effort. Furthermore, they appreciate JSC "Uzbekgidrenergo" and its connected organization "Tupalang GES" for providing historical bathymetric and other data.

Author contributions

Khojiakbar Khasanov: Conceptualization, Methodology, Software, Data curation, Visualization, Validation., **Masharif Bakiev:** Writing-Original draft preparation, Writing-Reviewing and Editing.

Conflicts of interest

The authors declare no conflicts of interest.

References

1. Otorbaev, D. (2022). Central Asia's Economic Rebirth in the Shadow of the New Great Game. London: Routledge. https://doi.org/10.4324/9781003360728
2. Abdullaev, I., & Akhmedov, S. (2022). Financing Infrastructure in Central Asia. In Unlocking Private Investment in Sustainable Infrastructure in Asia (pp. 72–88). London: Routledge. https://doi.org/10.4324/9781003228790-7
3. Yalçin, R., & Imagambetova, A. (2022). Problems of sharing transboundary water resources in Central Asia. Akademik Yaklaşımlar Dergisi, 13(2), 546–566. https://doi.org/10.54688/ayd.1111305
4. Tagbayev, A. (2022). Economic Activities and Traditional Activities of the Peoples of Central Asia are Highlighted in the Works of B.Kh. Karmisheva. International Journal of Social Science And Human Research, 05(10), 4770–4774. https://doi.org/10.47191/ijsshr/v5-i10-50
5. Şen, Z. (2021). Reservoirs for Water Supply Under Climate Change Impact—A Review. Water Resources Management, 35(11), 3827–3843. https://doi.org/10.1007/s11269-021-02925-0
6. Bakiev M, & Khasanov Kh. (2023). Determination of the capacity of the Kalkaman mudflow reservoir using geostatistical analysis. Irrigatsiya va Melioratsiya, 3(33), 18–26 (Russian).
7. Khasanov, K. (2024). A comprehensive analysis of reservoir capacity loss: a case study of the Akhangaran Reservoir, Uzbekistan. Water Cycle. https://doi.org/10.1016/j.watcyc.2024.11.003
8. Rakhmatullaev, S., Huneau, F., Le Coustumer, P., Motelica-Heino, M., & Bakiev, M. (2010). Facts and Perspectives of Water Reservoirs in Central Asia: A Special Focus on Uzbekistan. Water, 2(2), 307–320. https://doi.org/10.3390/w2020307
9. Wenhong, C. (2022). Sustainable sediment management for sustainable use of reservoirs. River, 1(2), 121–122. https://doi.org/10.1002/rvr2.26
10. Shaukat, N., Hashmi, A., Abid, M., Aslam, M. N., Hassan, S., Sarwar, M. K., … Tariq, M. A. U. R. (2022). Sediment load forecasting of Gobindsagar reservoir using machine learning techniques. Frontiers in Earth Science, 10. https://doi.org/10.3389/feart.2022.1047290
11. Bednar, M., & Marton, D. (2022). Reservoir sedimentation effect on water supply under conditions of climate change (pp. 181–190). https://doi.org/10.5593/sgem2022V/3.2/s12.21
12. Gonzalez Rodriguez, L., McCallum, A., Kent, D., Rathnayaka, C., & Fairweather, H. (2023). A review of sedimentation rates in freshwater reservoirs: recent changes and causative factors. Aquatic Sciences, 85(2), 60. https://doi.org/10.1007/s00027-023-00960-0
13. Sedláček, J., Bábek, O., Grygar, T. M., Lenďáková, Z., Pacina, J., Štojdl, J., … Elznicová, J. (2022). A closer look at sedimentation processes in two dam reservoirs. Journal of Hydrology, 605, 127397. https://doi.org/10.1016/j.jhydrol.2021.127397
14. Singh, R., L. Tiwari, H., & Singh, K. (2023). A GIS-Based Analysis for Reservoir Sedimentation. International Journal of Science and Research (IJSR), 12(10), 1057–1059. https://doi.org/10.21275/SR231013143411
15. Cimorelli, L., Covelli, C., De Vincenzo, A., Pianese, D., & Molino, B. (2021). Sedimentation in Reservoirs: Evaluation of Return Periods Related to Operational Failures of Water Supply Reservoirs with Monte Carlo Simulation. Journal of Water Resources Planning and Management, 147(1). https://doi.org/10.1061/(ASCE)WR.1943-5452.0001307
16. Walling, D. E. (2006). Human impact on land–ocean sediment transfer by the world's rivers. Geomorphology, 79(3), 192–216. https://doi.org/https://doi.org/10.1016/j.geomorph.2006.06.019
17. Li, Y., Zhao, G., Allen, G. H., & Gao, H. (2023). Diminishing storage returns of reservoir construction. Nature Communications, 14(1), 3203. https://doi.org/10.1038/s41467-023-38843-5
18. Zerihun, Y. T. (2023). A Study of the Sedimentation and Storage Capacity Depletion of a Reservoir. Slovak Journal of Civil Engineering, 31(2), 37–47. https://doi.org/10.2478/sjce-2023-0011
19. Mekonnen, Y. A., Mengistu, T. D., Asitatikie, A. N., & Kumilachew, Y. W. (2022). Evaluation of reservoir sedimentation using bathymetry survey: a case study on Adebra night storage

reservoir, Ethiopia. Applied Water Science, 12(12), 269. https://doi.org/10.1007/s13201-022-01787-0
20. Rakhmatullaev, S., Marache, A., Huneau, F., Le Coustumer, P., Bakiev, M., & Motelica-Heino, M. (2011). Geostatistical approach for the assessment of the water reservoir capacity in arid regions: a case study of the Akdarya reservoir, Uzbekistan. Environmental Earth Sciences, 63(3), 447–460. https://doi.org/10.1007/s12665-010-0711-3
21. Bist, M. S., Sonavane, A., Singh, A., Singh, J. K., & Selva Balan, M. (2023). A Capacity Loss and Silt Assessment of Khuga Reservoir, Manipur, Using Bathymetry Survey Technique—A Case Study' (pp. 431–438). https://doi.org/10.1007/978-981-19-9151-6_35
22. Wróbel, M., Mańk, K., Gawryś, R., Kaniewska, A. K., Boczoń, A., & Grajewski, S. (2023). The use of low-cost bathymetric methods for the purpose of exploiting mid-forest water reservoirs. International Journal of Hydrology Science and Technology, 16(1), 82–92. https://doi.org/10.1504/IJHST.2023.131835
23. Sichingabula, H., Chisola, M., Muchanga, M., Sikazwe, H., Chomba, I., & Phiri, W. (2022). Kaleya river catchment regional estimation of reservoir capacities using sonar and GIS approaches. Journal of Natural and Applied Sciences, 6(1), 1–13. https://doi.org/10.53974/unza.jonas.6.1.391
24. lhan Sercan, & Umut Aydar. (2023). Flood Analysis of Çan (Kocabaş) Stream With UAV Images. Advanced UAV, 3(1), 25–34.
25. Khasanov, K., & Ahmedov, A. (2021). Comparison of Digital Elevation Models for the designing water reservoirs: A case study Pskom water reservoir. In E3S Web of Conferences (Vol. 264). https://doi.org/10.1051/e3sconf/202126403058
26. Yakar, M., Yilmaz, H. M., & Yurt, K. (2010). The effect of grid resolution in defining terrain surface.Experimental Techniques, 34, 23-29. https://doi.org/10.1111/j.1747-1567.2009.00553.x.
27. Maraş, E. E., & Karafazlı, K. N. (n.d.). Monitoring coastal erosion and sediment accumulation in the Kızılırmak Delta using UAVs and photogrammetry. Advanced UAV, 2024(1), 42–52. http://publish.mersin.edu.tr/index.php/uav
28. Aghayev, A. (2018). Determining of different inundated land use in Salyan plain during 2010 the Kura River flood through GIS and remote sensing tools. International Journal of Engineering and Geosciences, 3(3), 80–86. https://doi.org/10.26833/ijeg.412348
29. Yağmur, N., Tanik, A., Tuzcu, A., Musaoğlu, N., Erten, E., & Bilgilioglu, B. (2020). Opportunities provided by remote sensing data for watershed management: example of Konya Closed Basin. International Journal of Engineering and Geosciences, 5(3), 120–129. https://doi.org/10.26833/ijeg.638669
30. Filippo Bandini, Daniel Olesen, Jakob Jakobsen, Cecile Marie Margaretha Kittel, Sheng Wang, Monica Garcia, & Peter Bauer-Gottwein. (2017). Technical note: Bathymetry observations of inland water bodies using a tethered single-beam sonar controlled by an unmanned aerial vehicle, Hydrol. Earth Syst. Sci., 22, 4165–4181, https://doi.org/10.5194/hess-22-4165-2018
31. Mujta, W., Wlodarczyk-Sielicka, M., & Stateczny, A. (2023). Testing the Effect of Bathymetric Data Reduction on the Shape of the Digital Bottom Model. Sensors, 23(12), 5445. https://doi.org/10.3390/s23125445
32. Parente, C., & Vallario, A. (2019). Interpolation of Single Beam Echo Sounder Data for 3D Bathymetric Model. International Journal of Advanced Computer Science and Applications, 10(10). https://doi.org/10.14569/IJACSA.2019.0101002
33. Shelke, S., Balan, S., & Kumar, C. (2016). Analysis of bathymetry data for calculating volume of water in a reservoir. In 2016 Conference on Advances in Signal Processing (CASP) (pp. 83–87). IEEE. https://doi.org/10.1109/CASP.2016.7746142
34. Vathar, S., & Shelke, S. (2016). Bathymetry data analysis and depth measurement. In 2016 Online International Conference on Green Engineering and Technologies (IC-GET) (pp. 1–5). IEEE. https://doi.org/10.1109/GET.2016.7916649
35. Akar, A. (2017). Evaluation of accuracy of DEMs obtained from UAV-point clouds for different topographical areas. International Journal of Engineering and Geosciences, 2(3), 110–117. https://doi.org/10.26833/ijeg.329717
36. Hastaoğlu, K. Ö., Göğsu, S., & Gül, Y. (2022). Determining the relationship between the slope and directional distribution of the UAV point cloud and the accuracy of various IDW interpolation. International Journal of Engineering and Geosciences, 7(2), 161–173. https://doi.org/10.26833/ijeg.940997
37. Tobler W, On the First Law of Geography: A Reply. Annals of the Association of American Geographers, 94(2), 304–310. https://doi.org/10.1111/j.1467-8306.2004.09402009.x
38. Loeffler, C. F., Lara, L. de O. C., & Ourique, F. R. (2022). Performance of spatial derivatives using interpolation with radial basis functions. STUDIES IN ENGINEERING AND EXACT SCIENCES, 3(4), 777–798. https://doi.org/10.54021/seesv3n4-014
39. Kamińska A., & Grzywna A. (2014). Comparison of deteministic interpolation methods for the estimation of groundwater level. Journal of Ecological Engineering, 15(4), 55–60. 10.12911/22998993.1125458

40. Bishop C. M., Neural networks for pattern recognition. Oxford university press, 1995. 10.1093/oso/9780198538493.001.0001
41. Yakar, M., & Dogan, Y. (2019). 3D Reconstruction of Residential Areas with SfM Photogrammetry. In Advances in Remote Sensing and Geo Informatics Applications: Proceedings of the 1st Springer Conference of the Arabian Journal of Geosciences (CAJG-1), Tunisia 2018 (pp. 73-75). Springer International Publishing.
42. Seddiki, A., & Dehimi, S. (2023). Effect of choosing a variogram model to predict salinity and its impact on the environment and geotechnical structures. Technium Social Sciences Journal, 39, 860–872. https://doi.org/10.47577/tssj.v39i1.8314
43. Zhang, Y., Pichon, L., Taylor, J. A., Oger, B., & Tisseyre, B. (2023). 82. Introducing Bayesian priors to semi-variogram parameter estimation using fewer observations. In Precision agriculture '23 (pp. 651–658). The Netherlands: Wageningen Academic Publishers. https://doi.org/10.3920/978-90-8686-947-3_82
44. Gribov, A., & Krivoruchko, K. (2020). Empirical Bayesian kriging implementation and usage. Science of The Total Environment, 722, 137290. https://doi.org/10.1016/j.scitotenv.2020.137290
45. Unel, F. B., Kusak, L., & Yakar, M. (2023). GeoValueIndex map of public property assets generating via Analytic Hierarchy Process and Geographic Information System for Mass Appraisal: GeoValueIndex. *Aestimum*, *82*, 51-69
46. Michael W. Mahoney, L. Johnson, Julia Silge, Hannah Frick, Max Kuhn, & Colin M. Beier. (2023). Assessing the performance of spatial cross-validation approaches for models of spatially structured data. https://doi.org/10.48550/arXiv.2303.07334
47. Yilmaz, A., & Erdoğan, M. (2018). Designing high resolution countrywide DEM for Turkey. International Journal of Engineering and Geosciences, 3(3), 98–107. https://doi.org/10.26833/ijeg.384822
48. Michael, S. (2010). A Comparison of Models and Methods for Spatial Interpolation in Statistics and Numerical Analysis. Georg-August-University Göttingen. https://doi.org/10.53846/goediss-2461
49. Karwariya, S., Dey, P., Bhogal, N. S., Kanga, S., & Singh, S. K. (2021). A Comparative Study of Interpolation Methods for Mapping Soil Properties: A Case Study of Eastern Part of Madhya Pradesh, India (pp. 431–449). https://doi.org/10.1007/978-3-030-76116-5_22
50. Castel, S., & S. Burr, W. (2021). Assessing Statistical Performance of Time Series Interpolators. In The 7th International conference on Time Series and Forecasting (p. 57). Basel Switzerland: MDPI. https://doi.org/10.3390/engproc2021005057
51. Ayana, E. K., Philpot, W. D., Melesse, A. M., & Steenhuis, T. S. (2014). Bathymetry, Lake Area and Volume Mapping: A Remote-Sensing Perspective. In Nile River Basin (pp. 253–267). Cham: Springer International Publishing. https://doi.org/10.1007/978-3-319-02720-3_14
52. Nagle, D.D., Campbell, B.G, and Lowery, M.A., (2009) Bathymetry of Lake William C. Bowen and Municipal Reservoir #1, Spartanburg County, South Carolina, 2008 (ver. 1.1, March 2015): U.S. Geological Survey Scientific Investigations Map 3076. https://dx.doi.org/10.3133/sim3076
53. Dourado, G. F., Hestir, E. L., & Viers, J. H. (2022). Establishing Reservoir Surface Area-Storage Capacity Relationship Using Landsat Imagery. In IGARSS 2022 - 2022 IEEE International Geoscience and Remote Sensing Symposium (pp. 863–866). https://doi.org/10.1109/IGARSS46834.2022.9884132
54. Francis, O. I., Anornu, G. K., Adjei, K. A., & Martin, E. O. (2021). Development of water surface area–storage capacity relationship using empirical model for Gurara reservoir, Nigeria. Modeling Earth Systems and Environment, 7(3), 2047–2058